TECHNICAL SCIENCES

METHODOLOGICAL APPROACHES TO STUDYING THE CRUSHING OF MICROPROJECTIONS IN CONTACT BETWEEN DISSIMILAR MATERIALS UNDER THERMAL DEFORMATION IMPACT

Abramov V.,
D.Sc.
Djagouri L.,
Prof., Eng.
Bogatov A.,
Student
Bogatov M.
Student
National Research University Moscow State University of Civil Engineering, Moscow, Russia; Pine Crest School, Fort Lauderdale, Florida 33334, USA
https://doi.org/10.5281/zenodo.15298399

Abstract

A methodology has been developed to study the contact interaction between dissimilar materials subjected to thermomechanical deformation over time. Kinetic curves were constructed to analyze contact formation, plastic deformation of microprojections, changes in microprojection height, contact stresses on microprojection contact areas, and variations in mechanical properties at the surface and within the near-contact volume of microprojections. These analyses were conducted across temperature ranges from room temperature to pre-melting points and pressure intervals before and after threshold values. The study demonstrates that plastic deformation of microprojections is responsible for contact formation and activation processes on contact surfaces. Additionally, the level of second-kind microstresses on microprojection contact areas significantly exceeds the nominal stress values used in calculation formulas. The research establishes that temperature and pressure have distinct effects on the intensity of plastic deformation, contact formation, and changes in mechanical properties at the surface and within the near-contact volume. The proposed process scheme enables the production of high-purity flat metal surfaces with adjustable mechanical properties and precision joints (both detachable and non-detachable).

Keywords: research methodology, contact interaction, microprojection crushing, kinetics, actual and physical contact, plastic deformation, sapphire, second-kind microstresses, smoothing, bonding.

1. Introduction

Advancements in science and technology impose increased demands on the geometry, strength, and reliability of machines, equipment, instruments, and devices, while maintaining their original physicochemical and mechanical properties during prolonged operation, including under extreme conditions and in aggressive environments. This necessitates the use of new materials or previously known materials in novel combinations. Consequently, there is a need to achieve precision detachable or non-detachable joints of these materials without altering their inherent properties.

One approach to addressing this issue is the study of contact interactions between materials in the solid phase under deformation or thermomechanical effects, leading to the development of new technological processes (TPs) for obtaining high-purity surfaces and precision joints without changing their original physicochemical and mechanical properties. Notably, TPs based on plastic deformation of microprojections on contact surfaces (such as pressure welding with heating, pressing and sintering of ultradispersed powders, obtaining high-purity metal surfaces with adjustable properties and geometry, etc.) play a significant role. These processes ensure efficiency by maximizing the preservation of the original material properties and regulating the precision of contact.

On one hand, precision joining involves not only controlling and regulating the deformation of the microrelief in the contact zone but also conducting preliminary treatment of contact surfaces using methods based on plastic reshaping through smoothing with natural and synthetic superhard materials. On the other hand, achieving a non-detachable precision joint requires understanding the kinetics and nature of processes occurring on contact surfaces under thermomechanical effects. This implies the need for direct experimental data on the kinetics of individual process stages, enabling the development of methods to control and regulate TPs for obtaining precision joints.

In this context, the problem of contact interaction under deformation or thermomechanical effects, encompassing joint formation, can be considered from two aspects:

1. Establishing kinetic patterns of contact formation between surfaces through plastic deformation of microprojections, considering changes in mechanical and elastic properties of the metal and surface geometry. This addresses the precision of the joint.
2. Investigating the activation nature of the surface of a harder material in contact with a softer metal and establishing kinetic patterns of bonding (strength growth) between them. This addresses the formation of a non-detachable precision joint.

Considering the problem of contact interaction from these aspects leads to the development of new TPs for obtaining precision detachable and non-detachable joints of materials in various combinations, including at temperatures below 0.5 of the metal's melting point, while preserving the original physicochemical and mechanical properties and geometry of the products.

The aim of this work was to establish the influence of thermomechanical impact levels on the nature of microprojection crushing during contact formation, the kinetics of contact development through plastic deformation of microprojections, changes in mechanical properties at the surface of contact pads and within the near-contact volume, as well as to assess the levels of second-kind microstresses compensated within the grain volume of microprojections under pressure welding with heating of dissimilar materials with sharply differing resistance to plastic deformation and chemical bonding nature.

2. Materials and Methods

The formation of a non-detachable joint during contact interaction of materials under pressure with heating is the result of several interrelated elementary processes, which, according to modern concepts, proceed in three main stages [1–3]:

1. the formation of physical contact;
2. the activation of atoms on the joining surfaces that are in physical contact and the formation of strong chemical (metallic) bonds;
3. the relaxation stage (formation of common grains, volumetric interactions, diffusion processes, etc.).

Due to the simultaneous occurrence of these processes in microscopic contact spots, conventional technological tests do not allow for a differentiated evaluation of the contribution of each stage to the overall joint formation. Therefore, identifying the development patterns of each process stage requires the use and development of specialized techniques and analytical calculation methods.

A number of studies [4–9] have experimentally examined the characteristics of elastic, plastic, and elastoplastic contact formation under varying parameters. However, there is a notable absence of works focused on the systematic study of the kinetics of actual contact formation, and its transition into physical contact, via the plastic deformation of microprojections on the welded surfaces. The qualitative and quantitative kinetic patterns of microprojection crushing at the contact interface have not been established, nor have the changes in mechanical properties at the surface of contact areas and within the microprojections. Additionally, the magnitudes of contact stresses within the microprojections, their kinetic evolution, and their fundamental role in activating the contact surfaces remain undetermined.

Furthermore, a significant discrepancy exists between experimental results and those predicted by existing models for individual process stages [3,7,10]. A common limitation of these models is that they rely on parameters of bulk creep deformation, while actual and physical contact formation occurs primarily due to plastic deformation of the microrelief features. This limitation has been compounded by the lack of a simple and objective methodology for systematically and accurately identifying the qualitative and quantitative patterns of contact formation, plastic deformation, microprojection crushing and reshaping—directly at the contact surfaces during pressure welding with heating and precision finishing treatments (smoothing) using synthetic superhard materials (SHMs).

Experimental investigations of the contact surfaces were performed using profilometry and fractography (optical and electron microscopy) on a fixed area [9]. The statistical processing of roughness parameter changes on the contact surfaces was conducted using a specialized computer program for the profilograph–profilometer model 201 with an integrated video computing system (IVK). The profilograph needle had a radius of 2 μm; vertical (VU) and horizontal (HU) magnifications ranged from 1,000 to 100,000 times and from 200 to 4,000 times respectively, with data automatically recorded onto thermoelectric paper.

Changes in mechanical properties on the surface of the contact pads and within the near-contact volume of the microprojections were assessed via microhardness (H) measurements using a PMT–3 device under a load of P = 0.5 N (50 gf). A fixed area on the test surface was marked using the diamond pyramid indenter of the PMT–3 instrument (Fig. 1 a–d) both before and after the application of the load. Profilograms were taken from the marked area pre- and post-loading. Control measurements of the height and base width of the microprojections were conducted using a MIS–11 dual microscope. An optical head from a binocular MBS microscope was used for observing and positioning the profilograph needle. After each loading cycle, the fixed area was photographed through sapphire.

The experimental studies were conducted on sample pairs of copper (MB grade) and synthetic monocrystalline optically transparent sapphire (corundum) with 600-orientation relative to the growth axis and a working surface finish of Rz = 0.03 μm. Sapphire was selected due to its highly favorable combination of properties relevant to practical applications—high hardness (9 on the Mohs scale), melting point, creep resistance, zero water absorption, and relative cost-effectiveness of production—all of which account for its broad use as a structural material in engineering [11–14].

This paper presents experimental results for the copper–sapphire pair. After mechanical processing, the copper samples were annealed in a hydrogen atmosphere at T = 650°C for 45 minutes. Contact surfaces were machined by turning (Rz = 3.2…6.3…10 μm) and planing (Rz = 40…80 μm). Sample dimensions were: length – 25 mm, diameter – 12 mm. The support surfaces of the samples were ground, and end face nonparallelism was no more than 0.002 mm. Loading was conducted using a diffusion welding setup of type A306.08. The vacuum level ranged from (1 to 5) × 10^{-5} mmHg. Temperature was measured with a chromel–alumel (CA) thermocouple, controlled by an MPShPr–54 device, and sealed beneath the base of the microprojection.

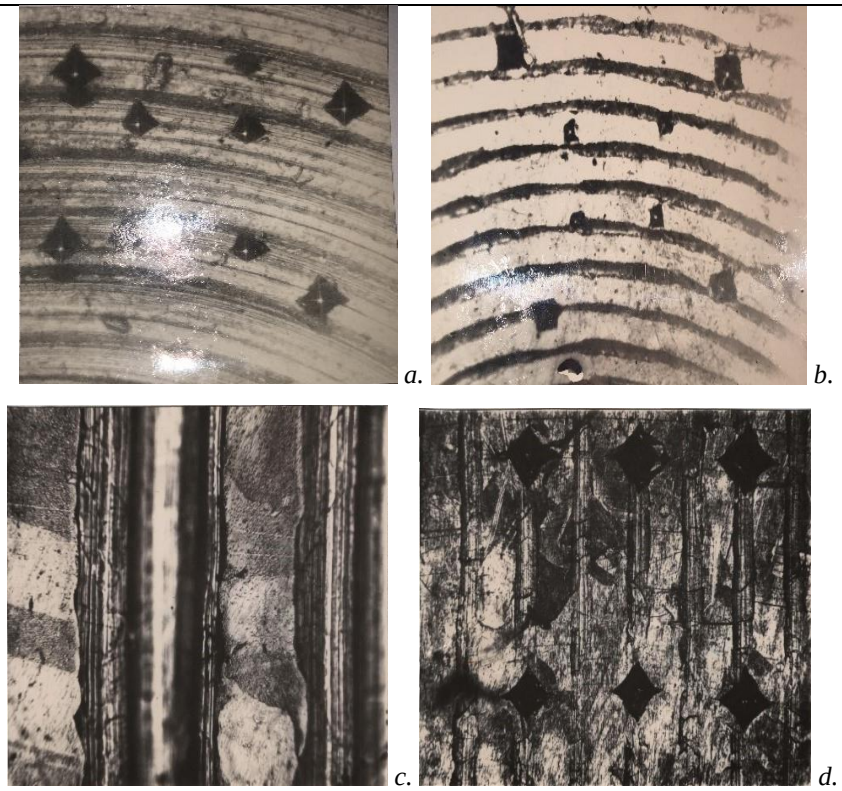

Fig. 1. Fractography of the contact surface before (a) and after (b, c, d) loading; surface treatment in (a, b) – turning, Rz = 3.2…6.3…10 μm; magnification ×110; (c, d) – planing, Rz = 40…80 μm; (a, b, c) – Stage 1 of microprojection crushing; (d) – Stage 2 of microprojection crushing.

Loading of the contact (welded) surface was carried out as follows. The specimen, mounted in a fixture (Fig. 2a), was placed inside a chamber where a vacuum was created and the system was heated to the process temperature. External (welding) pressure (P) was applied to the contact surface through a sapphire disc. The duration of the loading varied from 10…15…30 seconds to several tens of minutes, depending on the specific objectives of the smoothing or welding process. Thus, the process schemes for smoothing a metal surface with a flat sapphire disc and for welding under pressure with heating are similar, apart from certain technological differences [13–14].

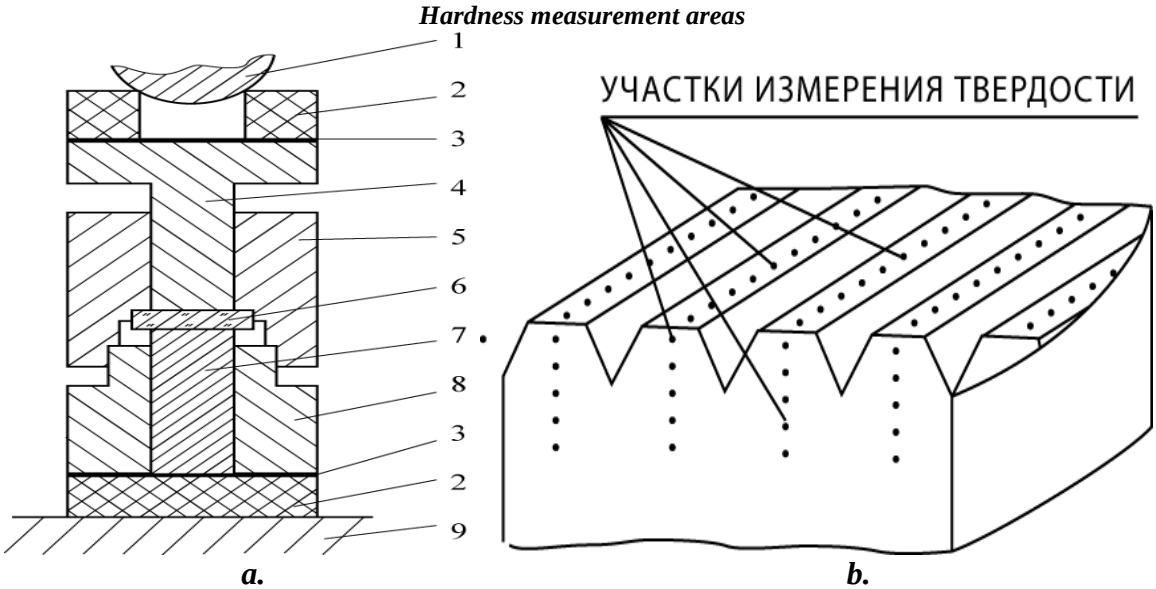

Fig. 2a, b.

Schematic diagram of the fixture for loading (a) and microhardness measurement (b) on the surface of the contact pads and into the depth of the microprojection.

Labels in Fig. 2a: 1 – ball, 2 – ceramic ring, 3 – mica, 4 – rod, 5 – sleeve, 6 – sapphire, 7 – test specimen, 8 – support sleeve, 9 – base support.

After holding the specimens in the fixture under specified temperature (T) and pressure (P), they were cooled to room temperature, and profilograms were again recorded from the fixed area using the same vertical (VU) and horizontal (HU) magnifications. By comparing the profilograms and processing them automatically with the IVK computer software, the relative amount of plastic deformation of the microprojections can be determined based on changes in their height (Fig. 3a, b), though only during the 1st and 2nd stages of microprojection crushing (see Fig. 4a, b). Additionally, by calculating the relative lengths (l_1, l_2, l_3 — see Fig. 3) of the contact pads within the designated fixed section (L), it is possible to determine the relative or absolute area of actual contact [17].

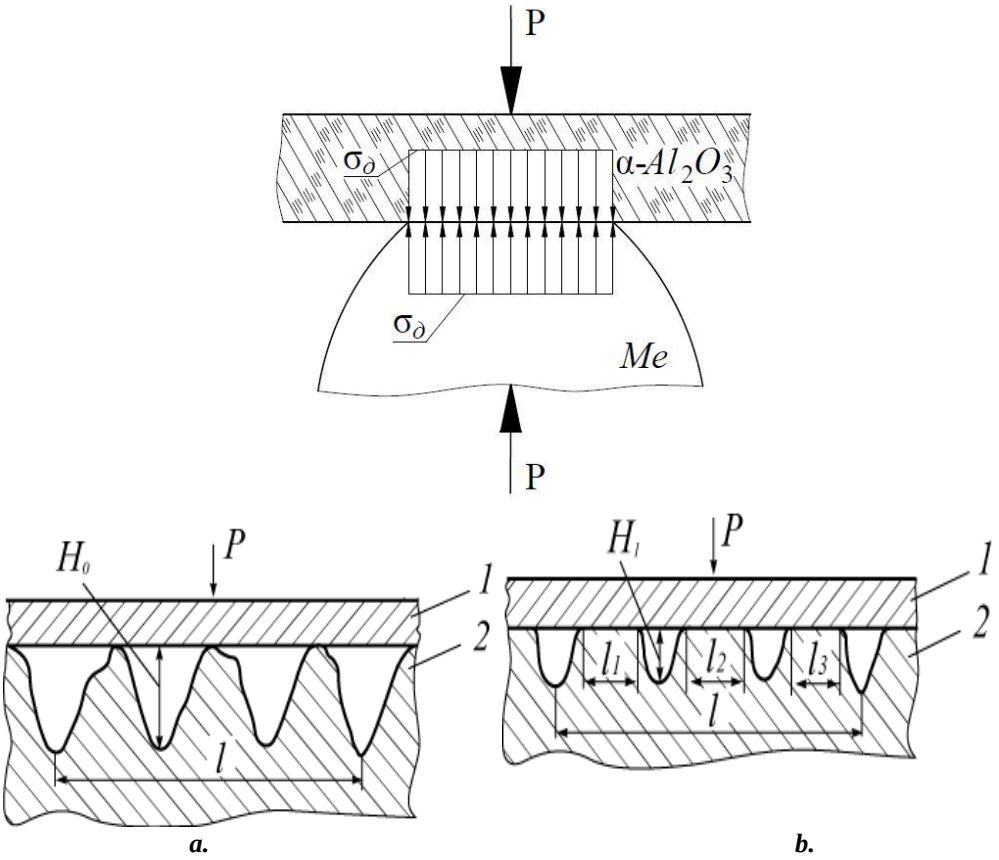

Fig. 3a, b.

Diagram of length (l) measurements on a designated section (L).
H_0 – initial height of microprojections; H_l – height at a given moment in time;
$l_{1,2,3}$ – width of contact pads, mm;
1 – corundum, 2 – metal.

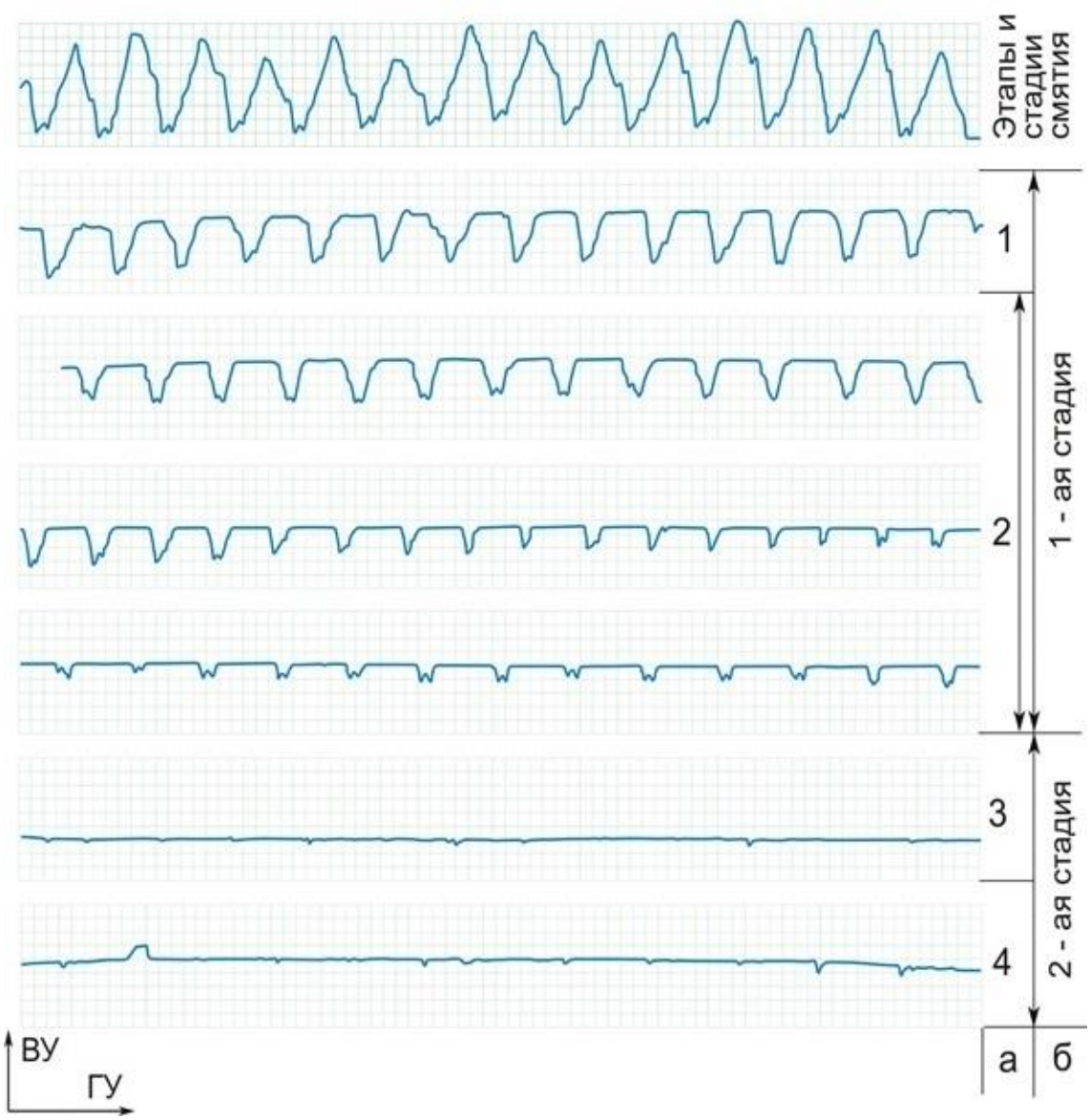

a.

Fig. 4a.
Character of the profilograms of copper contact surfaces after interaction with sapphire, showing four stages of microprojection crushing (a), and their consolidation into two stages (b).

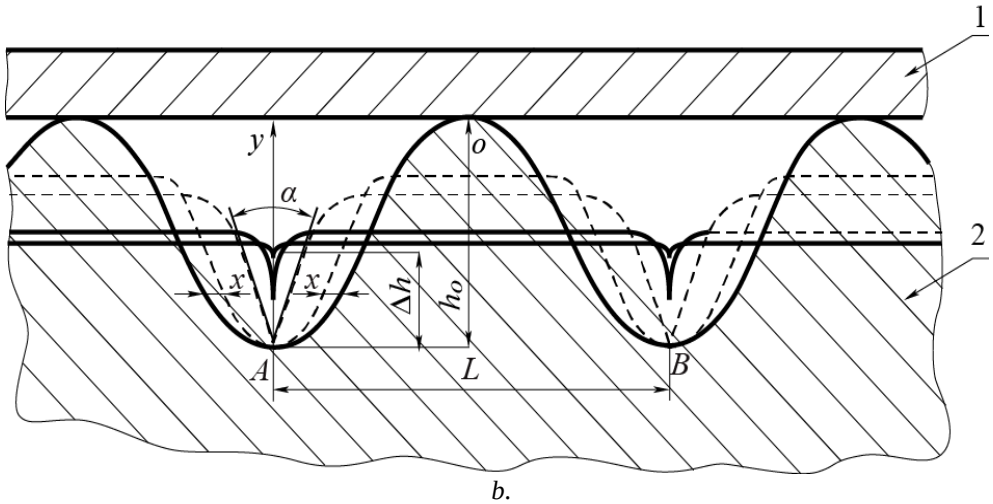

b.

Fig. 4b.
Diagram of the "apparent" rise of the lower point of the base of the microprojections on the flat surface during their crushing: 1 – sapphire; 2 – metal.

Mathematical processing of the obtained experimental results to assess the influence of (P, T, Rz) and time on the shape change of the microprojections, plastic deformation, and contact formation allowed for the derivation of an expression for calculating the formed contact area (F, mm²), namely:

$$F = \pi \cdot R^2 \cdot SF \quad (1)$$

Where:

- **R** – radius of the sample in mm,
- **S** – relative width of the contact areas (see Fig. 4), taking values (0 < S < 1).

Expression (1) allows for the calculation of the area of the formed contact at any stage of microprojection crushing during the finishing process of smoothing flat metal surfaces and their welding under pressure with heating, provided the relative width of the contact areas (determined experimentally via kinetics, i.e., this value is taken from the experimental graph of the functional dependence S = f (T, P, Rz)) and the sample radius (R) are known.

In our experiments, when processing contact surfaces by turning, the number of ring-shaped microprojections (n) ranged from 130 to 132, while by planing, n = 30 to 32. After simple transformations, we find that the calculated error in determining the shaded contact area (F) (see Fig. 5a, b) is approximately 1%. Using expression (1), the normal stresses (σ_d) in the contact between the microprojection and sapphire were calculated over the entire range of temperatures and pressures using the well-known expression:

$$\sigma_d = \frac{P}{F} \quad (2)$$

Kinetic curves showing the changes in normal (σ_d) and tangential (τ_d) stresses were constructed for each fixed moment of time.

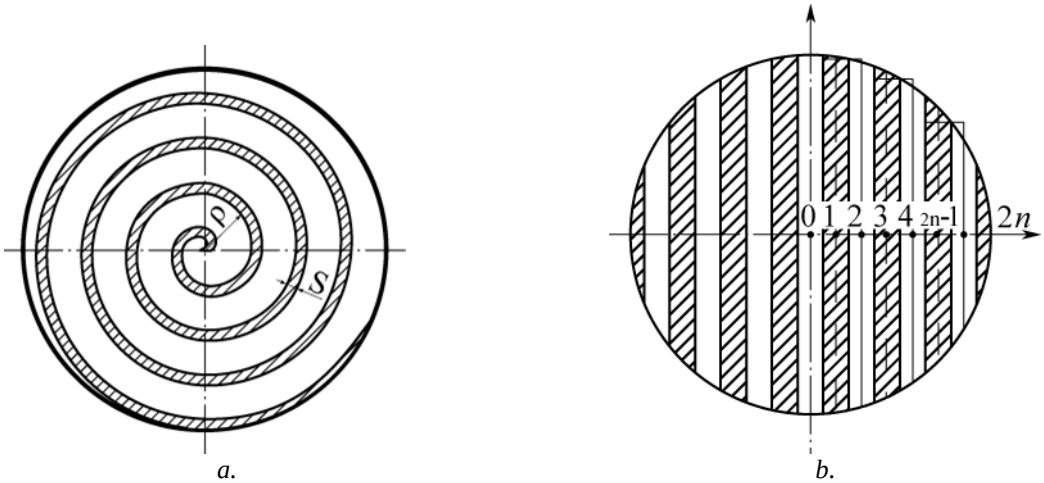

a. *b.*

Fig. 5a, b.
Diagrams for calculating the contact area F: (A – turning; B – planing)

3. Main Content of the Work

The use of profilographs and profilometers for obtaining information on changes in surface topography is limited by the physical capabilities of the method used. The key metrological characteristics of roughness measurement techniques are [15]:

- **Δz** – lower limit of measurement for the height of microprojections;
- **Δx, Δy** – spatial resolution of the field;
- **νmin and νmax** – frequency range limits of micron irregularities.

For profilographs, as well as for optical devices and methods for roughness control, the value of **Δz** is measured in hundredths of a micrometer, whereas the resolution in the field, **Δx,y**, is typically several times worse. This discrepancy can create the illusion of higher precision in measuring the "Z" coordinate of the real profile compared to the "X" and "Y" coordinates. In reality, this is not always the case, due to differences in the conditions for measuring microprojections during their crushing at different stages of the kinetic curve of contact formation and the presence of a correlation between **Δz** and **Δx,y**, which is established by the Ingelstam relationship [16]. Furthermore, the value **Δx,y ≠ 0** defines not only the upper limit of the measured frequencies of micron irregularities (**νmax = Δ⁻¹x,y**), but also introduces an additional systematic measurement error. This error depends not only on the class of accuracy of the profilograph but also on the surface relief characteristics and its temporal changes, which occur during solid-state welding under pressure with heating and during finishing smoothing [13, 14]. This component of the error is most significant in cases where the angle **α** at the apex of the microprojections (see Fig. 6a, b) is less than 90°. We will estimate the possible magnitude of this error and demonstrate that, in some cases, it can be excluded by a special method of processing the profilograms.

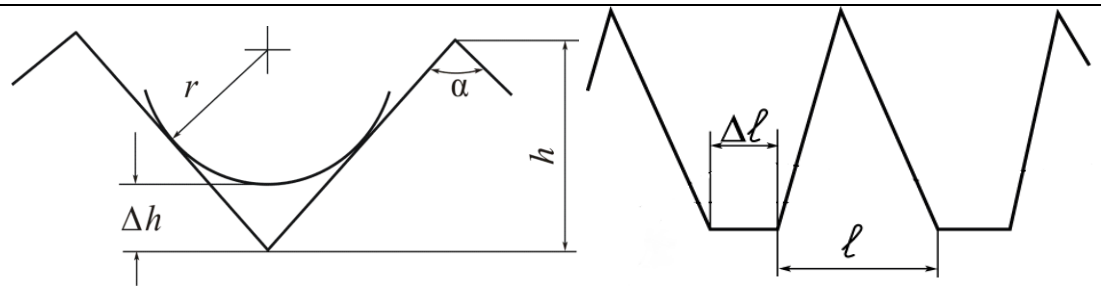

a *. b.*

Fig. 6. Scheme of the profile of microprojections on the contact surface.

Let's consider linear homogeneous micron irregularities created on the studied contact surface during its treatment with a triangular-section cutting tool with a sharpening angle **α**. The profile of such a surface can be approximated by the model shown in Fig. 6a. From geometric constructions, it is easy to see that the relative systematic error of profilograph measurement **Δh/h** is:

$$\frac{\Delta h}{h} = \frac{r \cdot (1 - \sin\frac{\alpha}{2})}{h \cdot \sin\frac{\alpha}{2}} = \frac{4 \cdot r \cdot \sin\frac{\alpha}{2} \cdot \left(1 - \sin\frac{\alpha}{2}\right)}{l \cdot \sin\alpha}$$

where: **r** – radius of the profilograph needle tip (**r = 2 μm** in our case).

As seen from the relationship (3), the measurement error is proportional to the ratio of **r/h** or **r/l**, and as the angle **α** decreases (while **h = const**), the error increases without bound. The relation (3) also shows the frequency dependence of the error **Δh/h**, since the value $\mathbf{l^{-1}}$ is the number of micron irregularities per unit length (the frequency of micron irregularities).

Numerical values of the measurement error, according to expression (3), for the specific case **r = 2 μm** and microprojection height **h = 10 μm**, reach **3%**, **8.5%**, and **20%**, respectively, for **α = 120°**, **90°**, and **60°**. The actual measurement accuracy can be higher due to rounding of the bottom of the pits between microprojections, but in all cases, these estimates are valid for micron irregularities spaced at a distance of about **Δx,y** or with small values of the angle **α**.

This error can be excluded by a special method of profilogram processing. This possibility is embedded in the methodology for determining the area of actual contact and the magnitude of plastic deformation of microprojections, based on comparing profilograms.

Typically, the relative deformation of microprojections **E_m** is found by comparing (see Fig. 3 or 4) the average initial height ($\mathbf{h_0}$) of the microprojections with their average height ($\mathbf{h_t}$) at the current moment in time (**t**) using the formula:

$$E_{\text{м}} = \left\{\frac{(h_0 - h_t)}{h_0}\right\} \cdot 100\%$$

However, the calculation of relative deformation of microprojections of welded surfaces during their group constrained settling does not account for the fact that, as the crushing process progresses, their side surfaces change (see Fig. 4), the angle between them decreases, and they weld together [8, 9, 12, 17]. To avoid the corresponding increase in the error of determining **E_m** using formula (4), we can use the relationship between the magnitude of **E_m** and the bearing part coefficient of the profile, which is numerically equal to the relative area of actual contact **S**, experimentally determined from profilograms by measuring the lengths of contact areas. The accuracy of measuring **S** is not significantly affected by the angle **α** at the apex of the microprojections.

Indeed, within the framework of the considered model of linear microprojections with triangular cross-sections, which become trapezoidal and rectangular as a result of their settlement, we will use the condition of mass and volume conservation of the microprojections.

This means that at all stages of microprojection compression, the cross-sectional area of the microprojections in the profilographing plane remains constant. Therefore, it follows that:

$$E_{\text{м}} = \frac{S}{(1+S)} \text{ or } \frac{\Delta h}{h_0} = \frac{1}{(1+S)}$$

Thus, the procedure for measuring $\mathbf{h_t}$ to find **E_m** can be replaced with the procedure for measuring **S** with high accuracy, thereby avoiding the inaccuracies in the measurement of the pit depth, which depends on the angle **α** and the established features and nature of the microprojection compression during their group settlement on the contact surfaces during pressure welding with heating and finish machining of metal surfaces with a flat sapphire tool [9, 12–14]. For the profile model that accounts for the "flatness" of the pit bottoms (Fig. 6b), expression (5) takes the form:

$$E_{\text{м}} = \frac{S \cdot \left(1 + \frac{\Delta l}{l}\right)}{\left[1 + S\left(1 + \frac{\Delta l}{l}\right)\right]}$$

As can be seen from the analysis of expressions (5) and (7), **S** is always greater than **E_m**, and as **S** approaches 1, **E_m** approaches 0.5. Whereas direct measurements of $\mathbf{h_t}$ of the microprojections and the estimation of the magnitude of plastic deformation **E_m** according to expression (4) lead to the conclusion that **E_m** is greater than **S**.

Therefore, comparing and analyzing the kinetics of the strength (bonding) of material joints with the kinetics of plastic deformation of microprojections during pressure welding with heating is incorrect and does not allow for an objective assessment of the process. Differentiating relations (5) and (7) allows us to find the rate (**Ė_m**) of plastic deformation of microprojections:

For the model (Fig. 5a):

$$\dot{E_{\text{м}}} = \frac{\dot{S}}{(1+S)^2}$$

For the model (Fig. 5b):

$$\dot{E_м} = \frac{\acute{S} \cdot \left(1 + \frac{\Delta l}{l}\right)}{\left[1 + S\left(1 + \frac{\Delta l}{l}\right)\right]^2}$$

Expressions (8) and (9) show that the relative area of actual contact (**S**) always increases significantly faster than the change in the magnitude of plastic deformation (**E_m**) of the microprojections on the contact surfaces. As an example, in Fig. 7a, b, the relationship between **E_m** and **S** is shown, and the kinetic curves of plastic deformation of microprojections during welding with heating of copper MB with sapphire and the formation of physical contact, calculated using formula (4), are compared with the features of compression (Fig. 7b) using formula (6) under the same welding and finishing parameters.

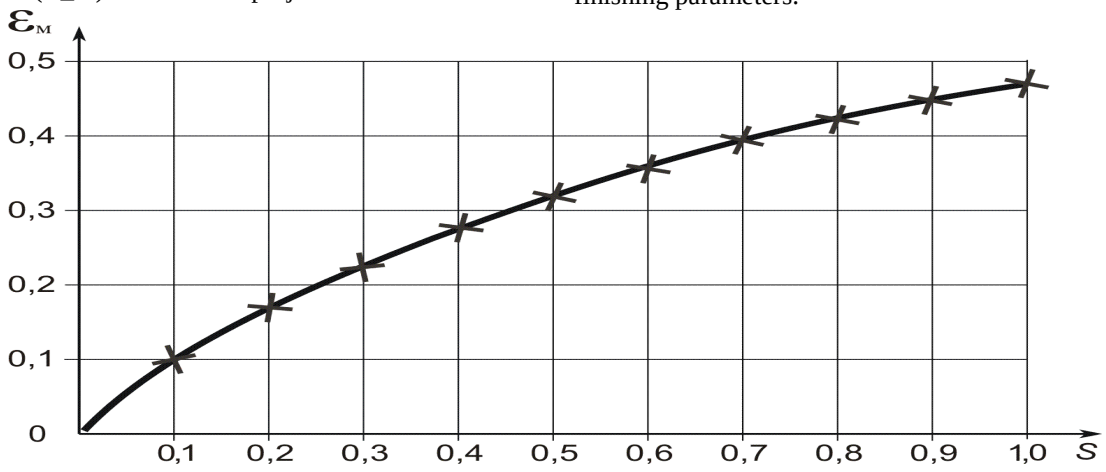

a.

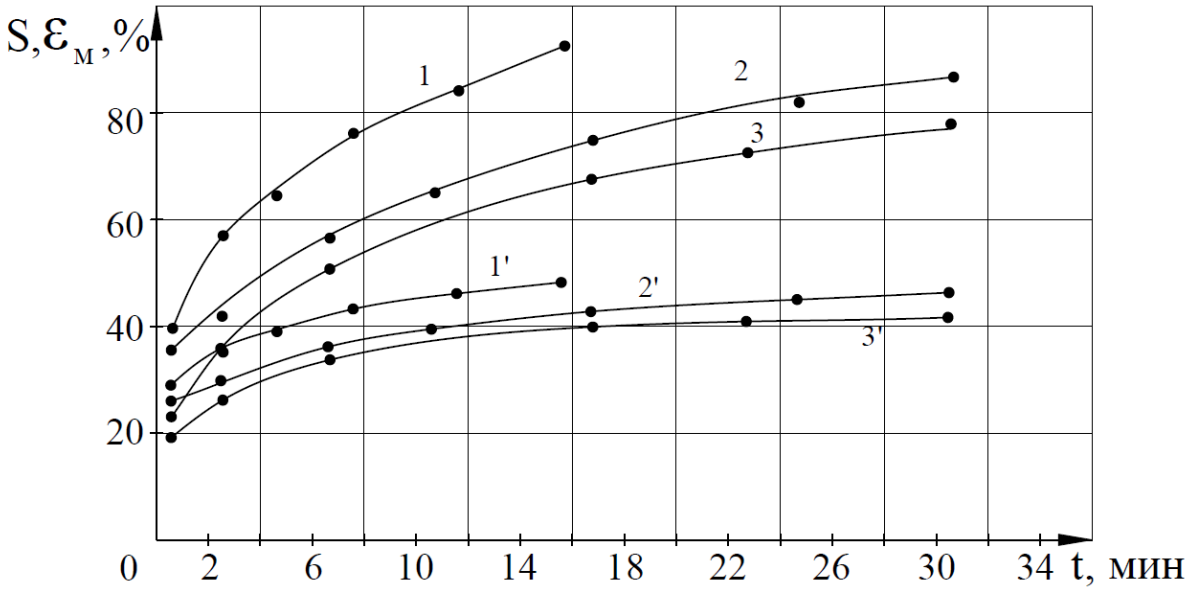

b.

Fig. 7.

a - Graphical relationship between the actual contact area (S) and the magnitude of relative plastic deformation (E_m) of the microprojections;

b - Comparison of the kinetic curves of the formation of physical contact S (1, 2, 3) and plastic deformation of the copper microprojections E_m (1', 2', 3') constructed using formula (5) accounting for the features of the compression of the microprojections; T_{sv} = 1173 K;

Curves:

1, 1' - 20 MPa; 2, 2' - 15 MPa; 3, 3' - 10 MPa; Rz = 40...80 μm.

This means that the kinetic curve of plastic deformation of microprojections should always lie below the kinetic curve of the formation of the actual contact as it reaches 0.6 of the nominal transition into physical contact during the second stage of the compression of microprojections [12,17]. Comparing and analyzing the kinetics of the strength growth (bonding) should be done with the kinetics of the development of contact areas (Fig. 8a, b, c) on plastically deforming microprojections, taking into account and based on the four stages of the compression of the microprojections, the developing micro-stresses of the second kind (normal σ_k and tangential τ_k), as well as the ongoing physical, chemical, and mechanical processes of the transfer of deformation from the "soft" metal to the harder body (sapphire) [19].

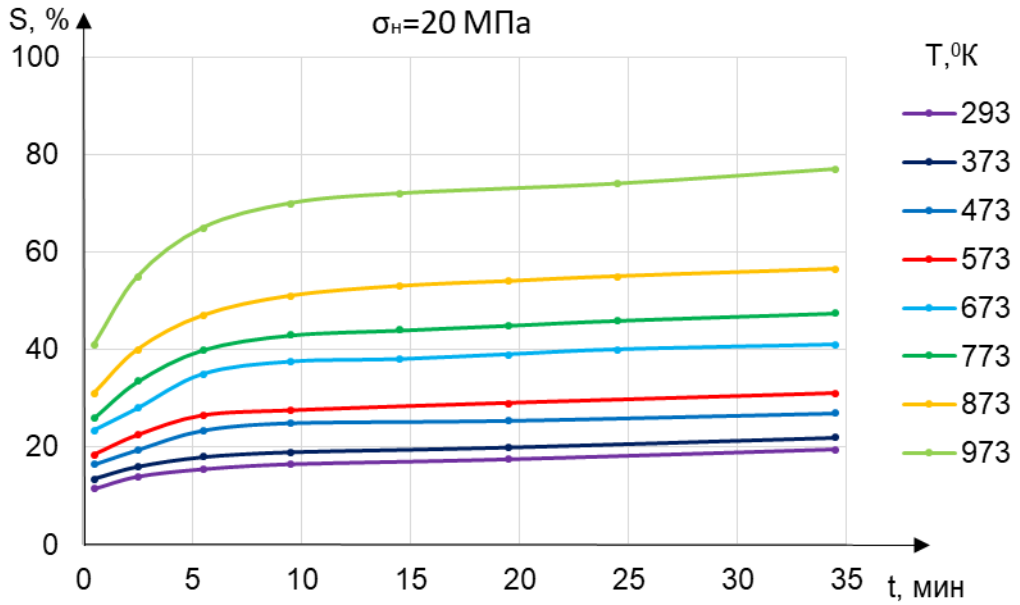

a.

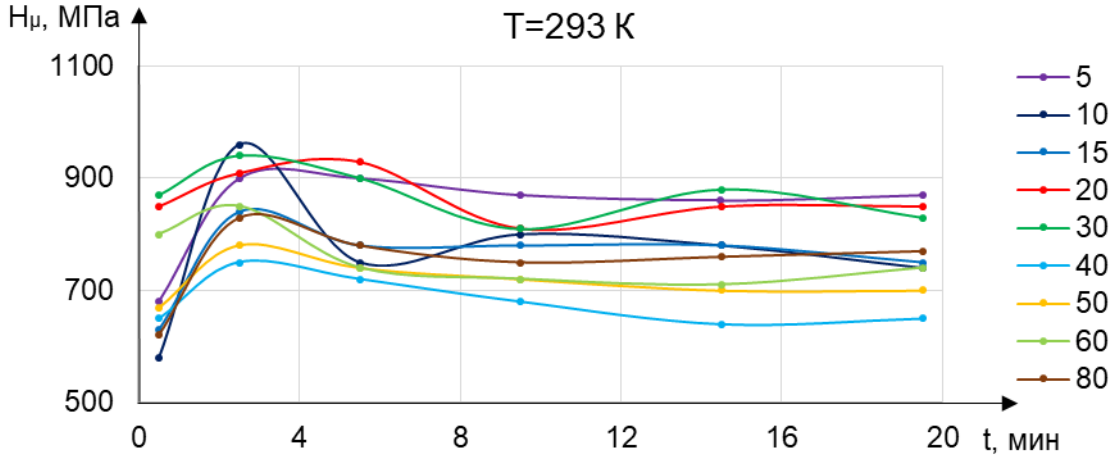

b.

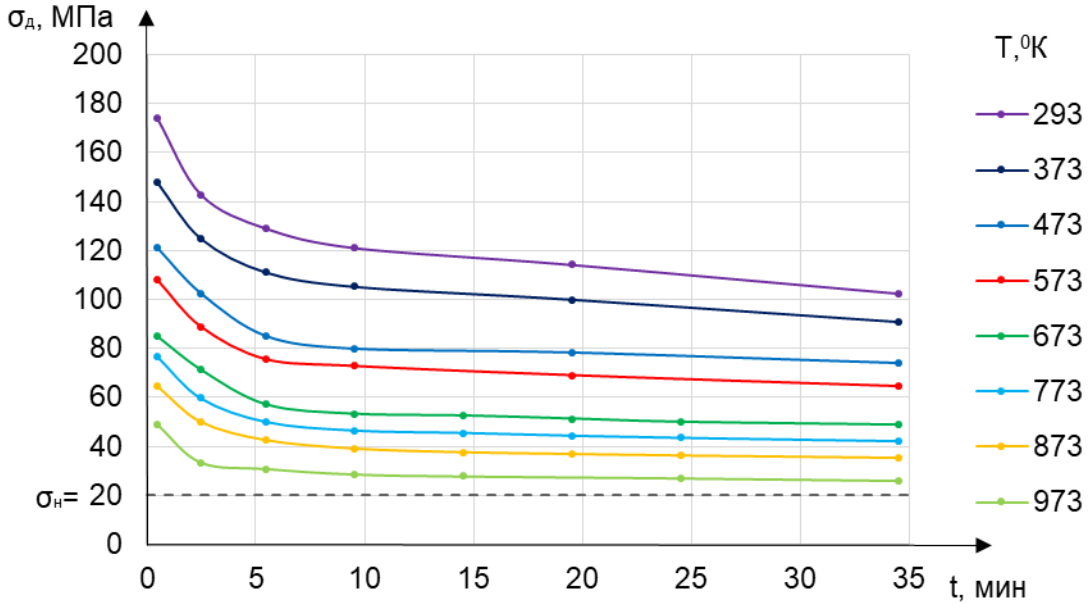

c.

Fig. 8 a, b, c. Kinetic curves of the formation of actual contact (a), changes in hardness on the surface of the contact areas (b), and changes in the acting normal stresses σ_k of second-kind microstresses (c).

It is important to consider that the size of a microasperity corresponds to the size of a single metal grain. This means that when calculating бд (σ_d) on each contact area of a microasperity, we determine the stresses compensated within the grain volume—i.e., second-kind microstresses. By recalculating them using known formulas, we determine the magnitude of the shear stresses of the second kind, also compensated within the grain volume [21,22]. By obtaining experimental values of S and substituting them into equation (8), the value of the relative plastic deformation (Ем) of the microasperities on the welded surfaces can be calculated.

Figure 7a shows the graphical relationship between the real contact area (S) and the relative plastic deformation (Ем) of the microasperities during pressure welding with heating and during fine finishing with a sapphire tool on flat surfaces.

4. Conclusions

The developed method for determining **Ем** and **S** was used to establish quantitative and qualitative patterns and the nature of microasperity deformation on contact surfaces of metals during fine finishing and the creation of surfaces with regulated and controlled mechanical properties, as well as during pressure welding with heating of dissimilar materials with sharply differing creep resistance.

This methodology also allows the calculation of the level of second-kind microstresses on the contact areas of microasperities and within their volume.

The conducted research explains the nature of the shift of the kinetic curve of strength growth (bond development) relative to the curve of physical contact formation between dissimilar materials. It also proposes a mechanism of relay-like deformation transfer from the "soft" metal grain to the harder one (sapphire), and the role of second-kind stresses in the initiation of submicroscopic cracks within the metal grain.

Additionally, this allowed an evaluation of the accuracy of previously published data by other authors concerning **Ем** as calculated using formula (4), which did not take into account the nature of microasperity deformation on the welded surfaces. It was confirmed that **Ем** is significantly overestimated when calculated using formula (4) based on direct measurements of **h**, with the error reaching up to **100%** as $\mathbf{S \rightarrow 1}$.

References:

1. **Rykalin N.N., Shorshorov M.Kh., Krasulin Yu.L.** Physical and chemical problems of bonding dissimilar materials. Proceedings of the USSR Academy of Sciences. Series: Inorganic Materials, 1965, No. 1, Issue 1, pp. 20–25.
2. **Krasulin Yu.L., Shorshorov M.Kh.** On the mechanism of bonding dissimilar materials in the solid state. Physics and Chemistry of Materials Processing, USSR Academy of Sciences, 1967, No. 1, pp. 15–18.
3. **Krasulin Yu.L.** Interaction of metal with a semiconductor in the solid phase. Moscow, Nauka, 1971, 120 pages.
4. **Mechanics and Physics of Contact Interaction.** Collection edited by N.B. Demkin, Kalinin Polytechnic Institute, Vol. 1, 1975, 165 pages; Vol. 2, 1976, 100 pages.
5. **Garkunov D.N.** The effect of wearlessness in friction. Scientific discoveries in tribology. Moscow, 2004, MSKhA Publishing, 383 pages.
6. **Kostetsky B.I.** Friction, lubrication, and wear in machines. Kyiv, Tekhnika, 1970, 395 pages.
7. **Shorshorov M.Kh., Krasulin Yu.L.** On the calculation of welding regimes under pressure. Welding Production, 1967, No. 7, pp. 15–21.
8. **Abramov V.V., Bychkova Z.S., Shorshorov M.Kh.** Kinetics of the topochemical reaction between copper and nickel during solid-phase welding. Physics and Chemistry of Materials Processing, 1972, No. 4, pp. 15–21.
9. **Abramov V.V.** Kinetics of plastic deformation of copper and nickel during solid-phase welding. Welding Production, 1973, No. 2, pp. 20–24.
10. **Karakozov E.S.** Bonding of metals in the solid phase. Moscow, Metallurgiya, 1976, 263 pages.
11. **Ruby and Sapphire.** Edited by M.V. Klassen-Neklyudova and Kh.S. Bagdasarov. Moscow, 1974, 236 pages.
12. **Kolmogorov G.D., Abramov V.V., Neretin N.A., et al.** Features of obtaining a non-detachable bond between monocrystalline sapphire and some metals by pressure welding with heating. Electronic Engineering, 1976, Series 7, No. 8, pp. 18–23.
13. **Author's Certificate No. 400488. USSR.** Moscow, Class B28d 5/00. Method for sealing sapphire windows. / N.V. Urusov, I.V. Babashov, G.V. Bondarenko, et al., 2 pages, Bulletin No. 40, 1973.
14. **Author's Certificate No. 350640. USSR.** Moscow, Class B24b 39/00. Finishing method. / N.V. Urusov, V.V. Abramov, V.N. Strel'nikov, et al., 2 pages, Bulletin No. 27, 1972.
15. **Kartashov A.I.** Surface roughness and methods of its measurement. Moscow, Standards Publishing, 1964, 163 pages.
16. **Ingel'shtamm D.** The principle of optical uncertainty and its application to quantitative information provided by multi-beam interferometers.
17. **Abramov V.V., Djagouri L.V.** Welding in construction and public utilities. Textbook in 2 volumes. Moscow, Granitsa, 2009, Vol. 1 – 413 pages, Vol. 2 – 519 pages.
18. **Pinegin S.V.** Contact strength and rolling resistance. Moscow, Mashinostroenie, 1969, 236 pages.
19. **Abramov V.V., Rakunov Yu.P., Suetina T.A., Gerasimenko V.B.** Technical foundations for the creation of machines and equipment for building materials enterprises. Moscow, MGAKhIS, Granitsa, 2009, 430 pages.